Journal of Chromatography, 236 (1982) 329–337
Elsevier Scientific Publishing Company, Amsterdam — Printed in The Netherlands

CHROM. 14,406

THERMODYNAMICS OF SOLUTIONS OF POLYCYCLIC AROMATIC HYDROCARBONS STUDIED BY GAS–LIQUID CHROMATOGRAPHY WITH A NEMATIC AND AN ISOTROPIC STATIONARY PHASE

G. M. JANINI* and M. T. UBEID
Department of Chemistry, Kuwait University, P.O. Box 5969 (Kuwait)
(First received August 13th, 1981; revised manuscript received September 22nd, 1981)

SUMMARY

Thermodynamic solution parameters of the isomeric polycyclic aromatic hydrocarbons phenanthrene and anthracene at infinite dilution in the nematic liquid crystal N,N′-bis(*p*-methoxybenzylidene)-α,α′-bi-*p*-toluidine (BMBT) and in its isotropic analogue N,N′-bis(*p*-methoxybenzylidene)-4,4′-diaminodiphenylmethane (BMBDM) have been derived by gas–liquid chromatography. The unique selectivity exhibited by BMBT towards isomeric polycyclic aromatic hydrocarbons is explained in the light of a current solution theory in terms of differences in the partial molar enthalpies and entropies of solution. Differences in solution behaviour between BMBT and BMBDM are examined with infinite-dilution solute activity coefficient, partial molar excess enthalpy and entropy data.

INTRODUCTION

Polycyclic aromatic hydrocarbons (PAHs) are ubiquitous in nature, being present in diverse environmental situations. Some of the most potent experimental carcinogens are members of this class of compounds[1]. Gas–liquid chromatography (GLC), particularly with open tubular columns coated with polymeric stationary phases such as SE-52, SE-30 and the Dexsil series, has been used, with various degrees of success, for the analysis of complex PAH mixtures[2,3]. However, the GLC separation of isomeric PAH mixtures has proved to be a difficult task. In particular, the separation of isomers such as phenanthrene/anthracene, benz[*a*]anthracene/triphenylene/chrysene and benzo[*a*]pyrene/benzo[*e*]pyrene/perylene/benzo[*k*]fluorenes were not satisfactory[4].

Nematic liquid crystals, on the other hand, show pronounced selectivities towards PAH isomers on the basis of differences in solute molecular shape. This unique solvent property of such phases is closely related to the long-range parallel alignment of their rod-like molecules, whereby rod-like solute molecules are preferentially accommodated while bulky solute molecules are discriminated against. Considerable interest has recently been shown in the use of liquid crystal stationary phases for practical analytical separations of PAH isomers and other classes of compounds[5–7].

0021-9673/82/0000–0000/$02.75

The theoretical interpretation of the separation mechanisms has not recieved as much attention since the prevailing "rule of thumb" that the more rod-like solute isomer should be retained longer in nematic phases does explain the order of retention in the majority of systems studied. It is to be emphasized that, while differences in solute shape are more or less the predominant factor in liquid crystal selectivity, other factors contributing to solubility (*e.g.*, dipole–dipole, dipole-induced dipole and charge transfer interactions if present) also play a part in the retention mechanisms. For example, the observed order of retention of isomeric methylbenz[*a*]anthracenes on a nematic stationary phase cannot be unambiguously explained solely on the basis of solute length-to-breadth ratio differences[8]. Moreover, the behaviour of PAH solutions in nematic solvents is more complex than that of rod-like molecules[9], because PAHs are biaxial plate-like molecules with two, rather than one, principal long molecular axes. It is, therefore, evident that detailed solution thermodynamic studies are needed in order fully to characterize the mechanism of retention of PAH solutes in nematic stationary phases.

GLC is a particularly attractive method for the investigation of solution thermodynamics of non-mesomorphic solutes in liquid crystal solvents. The ease with which data are obtained and the high level of accuracy make it the preferred technique for this type of study. The method has been successfully applied to solutions in nematic[10–15], smectic[16,17] and cholesteric[17,18] stationary phases. The results were generally interpreted according to a solution model originally proposed[10] and subsequently developed[19] by Martire and co-workers. In most of the studies cited the solutes were mainly low-molecular-weight aliphatics and disubstituted benzenes.

To our knowledge, the thermodynamics of solution of polycyclic aromatic hydrocarbons have never been studied on non-polymeric stationary phases, mesomorphic or otherwise. In this paper, GLC derived thermodynamic data, infinite-dilution activity coefficients, γ_2^∞, molar enthalpies, ΔH_2^∞, and entropies, ΔS_2^∞, of solution, partial molar excess enthalpies, H_2^∞, and entropies, S_2^∞, are reported for phenanthrene and anthracene on the nematic liquid crystal N,N′-bis(*p*-methoxybenzylidene)-α,α′-bi-*p*-toluidine (BMBT) and on its isotropic analogue N,N′-bis(*p*-methoxybenzylidene)-4,4′-diaminodiphenylmethane (BMBDM). The results of this study will be discussed in the light of Martire's solution model. Extension of this study to other PAH isomers was precluded because of the scarcity of needed solute vapour pressure and second virial coefficient data. It will be shown that the mechanisms of separation of plate-like molecules in nematic solvents are essentially similar to those proposed for rod-like molecules.

EXPERIMENTAL

Chemicals

The liquid crystal BMBT and its non-mesomorphic analogue BMBDM were synthesized as described in ref. 20. Both products were recrystallized twice from ethanol before use. The BMBT solid–nematic and nematic–isotropic phase transition temperatures were measured by differential scanning calorimetry at 181°C and 337°C, respectively. The solid–isotropic transition temperature for BMBDM occurs at 184°C. The phase transitions of BMBT coated on solid support were slightly lower than those of the bulk material.

The solutes studied were phenanthrene and anthracene. These were chosen as representatives of plate-like polycyclic aromatic hydrocarbons because of the availability of physical data (Table I) necessary for the derivation of thermodynamic quantities from GLC measurements. The solute vapour pressures, P_2^0, were calculated from the Antoine equation and the second virial coefficients, B_{22}, were computed from Kreglewski's equation (p. 47, ref. 21). The constants for these equations are available in ref. 21. Alternatively, B_{22} may be calculated from the equation of corresponding states of McGlashan and Potter[22], using available critical constants[21].

TABLE I

SOLUTE PHYSICAL PARAMETERS

Temperature (°C)	*Phenanthrene*			*Anthracene*		
	P_2^0 *(mmHg)*	$-B_{22}$* *(cm³ mol⁻¹)*		P_2^0 *(mmHg)*	$-B_{22}$* *(cm³ mol⁻¹)*	
190	15.86	5650	6738	15.50	5764	6628
200	22.61	5183	6232	22.03	5269	6131
210	31.67	4789	5777	30.76	4850	5685
220	43.60	4410	5368	42.23	4465	5283

* Values in the first column were calculated with the Kreglewski equation, those in the second with the McGlashan and Potter equation.

Preparation of columns

The packing material was prepared by coating BMBT and BMBDM on Chromosorb W HP (100–120 mesh) using the solvent slurry technique. A weighed amount of the liquid phase was dissolved or finely suspended in glass-distilled chloroform and transferred to a chloroform slurry of weighed solid support in a large evaporating dish. The excess of chloroform was initially removed in a rotatory evaporator and the slurry was dried in a drying oven at 60°C with gentle stirring. The dry packing material was resieved to the appropriate mesh specifications to ensure uniformity of particle size. The mass percent of liquid phase on the solid support was determined gravimetrically by ashing duplicate samples. Two columns (1.5 ft. × 0.25 in. copper tubing) were packed with each phase. The packed columns were conditioned at 230°C with a gentle flow of helium for about 3 h. Details of the column composition are given in Table II.

TABLE II

COMPOSITION OF COLUMNS

Column	*Liquid phase*	*Mass of packing (g)*	*% liquid phase*	*Mass of liquid phase (g)*
1	BMBDM	2.4659	11.96 ± 0.12	0.2949 ± 0.0029
2	BMBDM	2.5135	10.50 ± 0.11	0.2638 ± 0.0026
3	BMBT	2.7092	14.96 ± 0.15	0.4053 ± 0.0041
4	BMBT	2.4692	15.68 ± 0.16	0.3871 ± 0.0039

Apparatus and procedure

A Perkin-Elmer Sigma 1 gas chromatograph equipped with a dual-column, forced air oven, two flame ionization detectors, electronic carrier gas flow controllers and a Sigma 10 data station was employed. The column inlet pressure was measured with an auxiliary instrument pressure gauge accurate to ± 0.2 p.s.i., and column outlet pressure was read off a barometer. Oven temperatures were independently calibrated with a thermocouple. Temperature control at 200°C was accurate to ± 1.5°C. Retention data were directly recorded by the on-line data station. An average of three measurements was taken for each solute. The retention time of benzene (10 ± 2 sec at all temperatures) was used to correct for column dead-volume. At 220°C, the highest column temperature, this value was less than 2% of the retention time of phenanthrene. Minimum sample sizes were delivered as injections of generally less than 0.05 μl of solutions of solutes in benzene. All solute peaks were observed to be symmetrical and independent of sample size, indicating that infinte-dilution conditions have been satisfied. High liquid phase loadings on highly inert Chromosorb W HP were used in order to minimize any contribution to retention from adsorption of solute molecules on the solid support surface. Helium carrier gas flow-rates were read off the digital display, but were also checked at the column outlet with a calibrated soap-film meter.

RESULTS

Specific retention volumes, V_g^0, were obtained for both solutes at four well spaced temperatures in the nematic temperature region of BMBT, and at corresponding temperatures in isotropic BMBDM. The values reported in Table III represent the averages from two separate determinations on two columns each with different liquid phase loadings.

TABLE III

SPECIFIC RETENTION VOLUMES AND INFINITE-DILUTION ACTIVITY COEFFICIENTS

Solute	*Liquid phase*	V_g^0 ± 3%				γ_2 ± 3%			
		190°C	*200°C*	*210°C*	*220°C*	*190°C*	*200°C*	*210°C*	*220°C*
Phenanthrene	BMBT	719.0	532.0	397.0	300.6	3.33	3.17	3.03	2.91
Anthracene	BMBT	1013	736.0	539.5	401.7	2.43	2.35	2.31	2.25
Phenanthrene	BMBDM	2706	1923	1405	1045	0.917	0.905	0.885	0.866
Anthracene	BMBDM	2942	2075	1519	1118	0.863	0.861	0.845	0.836

V_g^0 is obtained from primary chromatographic data by the expression[15]

$$V_g^0 = t' \bar{F}_c^0 / g_1 \qquad (1)$$

where t' is the corrected solute retention time, $\bar{F}_c^0$ is the volume flow-rate of the carrier gas adjusted to the mean column pressure and 0°C and g_1 is the mass of liquid phase in the column.

The random errors reported for V_g^0 data represent the maximum scatter of the two experimental values from the mean. Authors[10–18] often cite an average random error in V_g^0 data of 1% or better. The higher uncertainty reported here is perhaps due to a larger than average error in g_1 and to poorer temperature control resulting from the use of the forced air oven at elevated temperatures. Examination of the results (Tables III–VI) clearly show that the important differences in the thermodynamic quantities are much larger than the error margin, allowing unqualified identification of the experimental trends.

The molar enthalpies, ΔH_2^s, and entropies, ΔS_2^s, of solution (Table IV) accompanying the infinte dilution transfer of solute (suscript 2) from its reference state (ideal gaseous mixture of solute plus carrier gas) to the real solution (both gaseous and liquid phases being at the same temperature and pressure) are obtained from the expression[23]

$$\ln V_g^0 = \frac{-\Delta H_2^s}{RT} + \frac{\Delta S_2^s}{R} + \ln\left(\frac{273.2\ R}{M_1}\right) \tag{2}$$

where M_1 is the molar mass of the liquid phase. The correlation coefficients of the linear regression of average ln V_g^0 *vs.* reciprocal temperature were all in excess of 0.999.

TABLE IV

SOLUTE THERMODYNAMIC DATA

Solute	*Liquid phase*	$-\Delta H_2^s$ (*kJ mol*$^{-1}$)	$-\Delta S_2^s$ (*J K*$^{-1}$ *mol*$^{-1}$)	H_2^e (*kJ mol*$^{-1}$)	S_2^e (*J K*$^{-1}$ *mol*$^{-1}$)
Phenanthrene	BMBT	55.3 ± 1.7	78.1 ± 2.3	8.57	8.51
Anthracene	BMBT	58.7 ± 1.8	82.6 ± 2.5	4.60	2.59
Phenanthrene	BMBDM	60.2 ± 1.8	78.0 ± 2.3	3.64	8.56
Anthracene	BMBDM	61.1 ± 1.8	79.3 ± 2.4	2.18	5.92

Infinite dilution solute activity coefficients, γ_2^∞, were calculated from V_g^0 data via[15]

$$\ln \gamma_2^\infty = \ln\left(\frac{273.2\ R}{M_1 P_2^0 V_g^0}\right) - \frac{B_{22} P_2^0}{RT} \tag{3}$$

where all the terms are as defined earlier and the B_{22} values are those determined by Kreglewski's equation. The resulting γ_2^∞ values are listed in Table III. The virial coefficients may, alternatively, be calculated with the McGlashan and Potter equation[22], but since the total fugacity correction, $B_{22}P_2^0/RT$, contributes less than 1.5% to the corresponding γ_2^∞ values, it is immaterial which approximate B_{22} values are used. It is to be noted that the relative standard deviations in the slopes and intercepts of the ln V_g^0 *vs.* $1/T$ plots are all less than ± 1%. However, since the accuracy of the derived ΔH_2^s, ΔS_2^s and γ_2^∞ values primarily depends on the accuracy of the V_g^0 data, the uncertainties in these quantities are essentially not better than those reported for V_g^0.

The thermodynamic relationship between the activity coefficient at infinite dilution and the solution partial molar excess properties is given by

$$\ln \gamma_2^{\infty} = \frac{G_2^E}{RT} = \frac{H_2^E}{RT} - \frac{S_2^E}{R} \tag{4}$$

where G_2^E, H_2^E and S_2^E are, respectively, the infinite dilution partial molar excess Gibbs energy, enthalpy and entropy of solution. A linear regression analysis of $\ln \gamma_2^{\infty}$ *vs.* reciprocal temperature yields H_2^E from the slope and S_2^E from the intercept. Plots of $\ln \gamma_2^{\infty}$ *vs.* $1/T$ are shown in Fig. 1, and the resulting H_2^E and S_2^E values are listed in Table IV. All correlation coefficients were in excess of 0.996, but the relative standard deviations in H_2^E and S_2^E are essentially the same as those for ΔH_2^E and ΔS_2^E respectively.

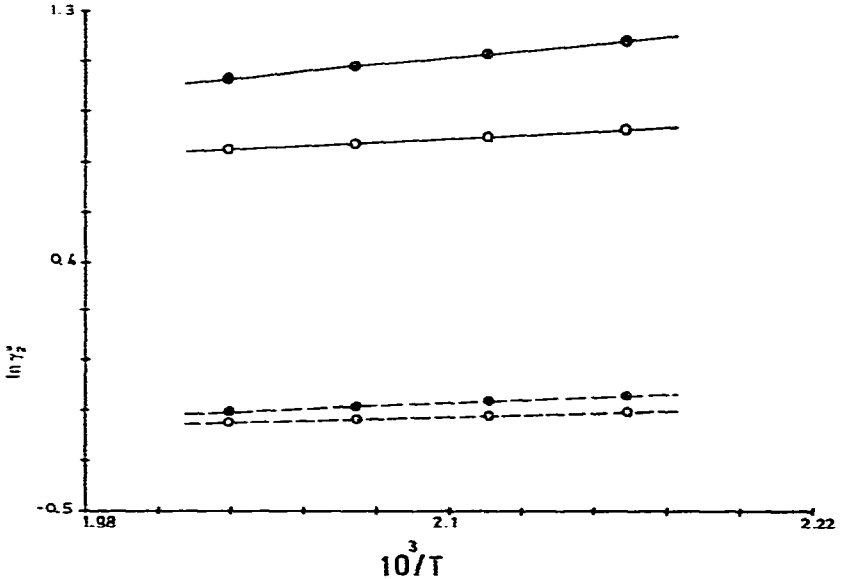

Fig. 1. Plots of $\ln \gamma_2^{\infty}$ *vs.* $10^3/T$ for phenanthrene (●) and anthracene (○) in BMBT (———) and BMBDM (– – –).

Furthermore, ΔH_2^E is related to H_2^E through the thermodynamic relation

$$\Delta H_2^E = H_2^E - \Delta H_2^V \tag{5}$$

where ΔH_2^V is the molar enthalpy of vaporization of the pure solute. ΔH_2^V values were calculated for both phenanthrene and anthracene using eqn. 5 with data from Table IV, and the results were compared with literature values (Table V). The excellent agreement reflects the quality of the data.

The mechanisms of retention of polycyclic aromatic hydrocarbons in nematic solvents could be studied via the temperature dependence of the relative retention, α,

TABLE V

COMPARISON OF GLC-DERIVED ENTHALPIES OF VAPORIZATION WITH LITERATURE VALUES

Solute	*Liquid phase*	ΔH_2^v *(experimental)* *(kJ mol^{-1})*	ΔH_2^v *(literature)** *(kJ mol^{-1})*
Phenanthrene	BMBT	63.83	63.43
	BMBDM	63.83	
Anthracene	BMBT	63.27	63.01
	BMBDM	63.27	

* Calculated average value at the four experimental temperatures: 190, 200, 210 and 220°C, with data from ref. 21.

of isomeric solute pairs[15]. The relevent equation for the solute pair phenanthrene (P) and anthracene (A) is simply derived from the basic definition:

$$\alpha(\mathrm{A/P}) = (V_g^0)_A/(V_g^0)_P \tag{6}$$

It follows from eqn. 2 that:

$$\ln \alpha\,(\mathrm{A/P}) = \frac{-\Delta H_A^s + \Delta H_P^s}{RT} + \frac{\Delta S_A^s - \Delta S_P^s}{R} = \frac{\Delta(\Delta H^s)_{P-A}}{RT} - \frac{\Delta(\Delta S^s)_{P-A}}{R} \tag{7}$$

where $\Delta(\Delta\ )_{P-A}$ indicates the value for phenanthrene minus that for anthracene. $\Delta(\Delta H^s)_{P-A}$ and $\Delta(\Delta S^s)_{P-A}$ values may be obtained directly from data in Table IV, or from the slopes and intercepts of plots of ln α (A/P) *vs.* $1/T$. The two procedures yield identical results in nematic BMBT liquid phase where the α(A/P) values are large. In contrast, the correlation coefficient for the α(A/P) *vs.* $1/T$ plot in isotropic BMBDM is poor and, therefore, the results presented in Table VI are those calculated from data in Table III.

TABLE VI

RELATIVE RETENTION AND DIFFERENCES IN ENTHALPY AND ENTROPY OF SOLUTION BETWEEN ANTHRACENE AND PHENANTHRENE

Solute pair	*Liquid phase*	α *(A/P)*				$\Delta(\Delta H^s)_{P-A}$ *(kJ mol^{-1})*	$\Delta(\Delta S^s)_{P-A}$ *(J K^{-1} mol^{-1})*
		190°C	*200°C*	*210°C*	*220°C*		
A–P	BMBT	1.408	1.383	1.359	1.336	3.40	4.50
A–P	BMBDM	1.087	1.079	1.081	1.070	0.90	1.30

DISCUSSION

First we consider the factors affecting the selectivity of nematic BMBT towards PAH isomers in the light of a theoretical model initially developed[10] and later modified[19] by Martire and co-workers. According to this model, the main sources of deviation from ideality for solutions of rigid isomers in a nematic solvent are rotational and energetic. Furthermore, these two contributions are mutually dependent as confirmed by a recent extension of the Maier-Saupe theory[24]. According to this theory, solute–nematic solvent interactions depend on the shape of the solute molecule, being stronger for a more rod-like solute which is better accommodated in the ordered nematic domain. As a consequence of this greater orientational order, the more rod-loke solute suffers a greater loss of translational and rotational motion than a bulkier isomer.

When comparing the solution behaviour of a pair of solutes in a common solvent the most appropriate thermodynamic quantities to consider are $\Delta(\Delta H_2^s)$ and $\Delta(\Delta S_2^s)$, as they are a direct measure of the differences in solute–solvent interactions (solute–solute interactions are absent in these terms, and solvent–solvent interactions cancel out with a common solvent). For solutions of phenanthrene and anthracene in BMBT, we find that $\Delta(\Delta H^s)_{P-A}$ represents the difference (phenanthrene minus anthracene) in the strengths of the solute–solvent interactions, while $\Delta(\Delta S^2)_{P-A}$ reflects the compatibility of the solute with the solvent domain.

The results presented in Table VI show that $\Delta(\Delta H^s)_{P-A}$ and $\Delta(\Delta S^s)_{P-A}$ values are all positive and significantly larger on BMBT compared to isotropic BMBDM. A positive $\Delta(\Delta H^s)_{P-A}$ results from a more negative ΔH^s for anthracene, indicating stronger solute–solvent interactions for this isomer. Since intermolecular interactions for both anthracene and phenanthrene with the same nematic solvent are expected to be of the same nature (*i.e.*, same potential energy curve), it can safely be assumed that anthracene–solvent interactions operate at shorter average distances than those of phenanthrene. The positive $\Delta(\Delta S^s)_{P-A}$ values add further credence to this assumption since the greater orientational order imposed on anthracene results in greater loss of its translational and rotational entropy. The fact that anthracene is invariably retained on BMBT longer than phenanthrene indicates that the favourable enthalpic enhancement of solubility outweighs the unfavourable entropic factor. As the temperature is increased, the difference in α(A/P) values on BMBT compared to BMBDM diminishes and α(A/P) values decrease. In BMBDM, $\Delta(\Delta H^s)_{P-A}$ and $\Delta(\Delta S^s)_{P-A}$ are quite small and the α(A/P) values are close to unity. This clearly indicates that it is the orientational order in BMBT that is responsible for the solute shape-dependent selectivity. It is concluded that the mechanisms of separation of phenanthrene/anthracene, and of other PAH isomers, are essentially the same as those proposed for rigid rod-like molecules[15].

Finally, we collate the solution properties of nematic BMBT and isotropic BMBDM at the same experimental temperatures. It has repeatedly been demonstrated that liquid crystals are relatively poorer solvents in their nematic regions compared to their isotropic melts[10–15]. Typically, V_g^0 is smaller and γ_2^∞ is more positive at a given temperature in the nematic state than the corresponding values extrapolated to the same temperature from the isotropic state. However, this type of comparison is not feasible with liquid crystals having high nematic–isotropic transition temperatures.

BMBT columns, for example, exhibit excessive bleeding and liquid phase deterioration at high temperatures, rendering impossible the collection of relevant chromatographic data in the isotropic region at temperatures greater than 337°C. Furthermore, the temperature region of prime importance in practical GLC separations is that immediately above the solid–nematic transition temperature[5]. To circumvent this problem, non-mesomorphic BMBDM was chosen for this type of comparison. It is ideally suited for this purpose since it is analogous to BMBT in chemical structure except for one less methylene group in the central linkage.

Examination of the data in Tables III and IV reveals that for a given solute in BMBT solvent, $\gamma_2^\infty > 1$, $H_2^s > 0$ and $S_2^s > 0$. Positive S_2^s indicate higher solubility, but it is clear that this favourable entropic factor is overwhelmed by the unfavourable positive H_2^s contribution as $\gamma_2^\infty > 1$. This relatively large positive deviation from ideality is attributed to the incompatability of the non-mesomorphic solute in the ordered solvent domain. The bulkier the solute, the more incompatible it is in the nematic solvent. This explains the more positive γ_2^∞, H_2^s and S_2^s values for the phenanthrene isomer in BMBT. In contrast, both solutes exhibit negative deviations from ideality in isotropic BMBDM ($\gamma_2^\infty < 1$) as the excess entropic contribution slightly outweighs the excess enthalpic effect. Isotropic BMBDM is, therefore, a much better solvent for this class of compounds, but nematic BMBT is a far more selective liquid phase for the separation of PAH isomers.

ACKNOWLEDGEMENT

This research was sponsored by the College of Graduate Studies, Kuwait University.

REFERENCES

1 A. Dipple, *Excerpta Med. Int. Congr. Ser. 350*, Vol. 2. *Chemical and Viral Oncogenesis*, 1974.
2 M. L. Lee and B. W. Wright, *J. Chromatogr. Sci.*, 18 (1980) 345.
3 H. Borwitzky and G. Schomburg, *J. Chromatogr.*, 170 (1979) 99.
4 G. M. Janini, K. Johnston and W. L. Zielinski, Jr., *Anal. Chem.*, 47 (1975) 670.
5 G. M. Janini, *Advan. Chromatogr.*, 17 (1979) 231.
6 W. L. Zielinski, Jr. and G. M. Janini, *J. Chromatogr.*, 186 (1979) 237
7 H. Kelker, *Advan. Liq. Cryst.*, 3 (1978) 237.
8 G. M. Janini, R. I. Sato and G. M. Muschik, *Anal. Chem.*, 52 (1980) 2417.
9 R. Alben, *J. Chem. Phys.*, 59 (1973) 4299.
10 L. C. Chow and D. E. Martire, *J. Phys. Chem.*, 75 (1971) 2005.
11 D. G. Willey and G. H. Brown, *J. Phys. Chem.*, 76 (1972) 99.
12 A. A. Jeknavorianand E. F. Barry, *J. Chromatogr.*, 101 (1974) 299.
13 J. F. Bocquet and C. Pommier, *J. Chromatogr.*, 117 (1976) 315.
14 G. A. Oweimreen, G. C. Lin and D. E. Martire, *J. Phys. Chem.*, 83 (1979) 2111.
15 D. E. Martire, A. Nikolić and K. L. Vasanth, *J. Chromatogr.*, 178 (1979) 401.
16 H. Kelker, *Ber. Bunsenges. Phys. Chem.*, 67 (1963) 698.
17 D. E. Martire, P. A. Blasco, P. F. Carone, L. C. Chow and Vicini, *J. Phys. Chem.*, 72 (1968) 3489.
18 J. M. Schnur and D. E. Martire, *Mol. Cryst. Liq. Cryst.*, 26 (1974) 213.
19 D. E. Martire, *Mol. Crust. Liq. Cryst.*, 28 (1974) 63.
20 G. M. Janini, G. M. Muschik and C. M. Hanlon, *Mol. Crust. Liq. Cryst.*, 53 (1979) 15.
21 *API Monograph Series*, Publication 708, American Petroleum Institute, Washington, DC, 1979.
22 M. L. McGlashan and D. J. B. Potter, *Proc. R. Soc. London, Ser. A*, 267 (1962) 478.
23 E. F. Meyer, *J. Chem. Educ.*, 50 (1973) 191.
24 D. E. Martire, in G. R. Luckhurst and G. W. Gray (Editors), *The Molecular Physics of Liquid Crystals*, Academic Press, London, 1979, Ch. 11.